Cardiovasc Intervent Radiol
DOI 10.1007/s00270-009-9595-6

CLINICAL INVESTIGATION

Hepatocellular Carcinoma Supplied by the Right Lumbar Artery

Shiro Miyayama · Masashi Yamashiro · Miho Okuda · Yuichi Yoshie · Natsuki Sugimori · Saya Igarashi · Yoshiko Nakashima · Osamu Matsui

Received: 23 March 2009 / Accepted: 23 April 2009

Abstract This study evaluated the clinical features of hepatocellular carcinoma (HCC) supplied by the right lumbar artery. Eleven patients with HCC supplied by the right lumbar artery were treated with chemoembolization. The patients' medical records were retrospectively analyzed. All patients underwent 6.7 ± 3.7 (mean ± SD) chemoembolization sessions, and the hepatic arterial branches were noted as being attenuated. The right inferior phrenic artery (IPA) was also embolized in 10 patients. The interval between initial chemoembolization and chemoembolization of the lumbar artery supply was 53.2 ± 26.9 months. Mean tumor diameter was 3.1 ± 2.4 cm and was located at the surface of S7 and S6. The feeding-branch arose proximal to the bifurcation of the dorsal ramus and muscular branches ($n = 8$) or from the muscular branches ($n = 3$) of the right first ($n = 10$) or second lumbar artery ($n = 1$). The anterior spinal artery originated from the tumor-feeding lumbar artery in one patient. All feeders were selected, and embolization was performed after injection of iodized oil and anticancer drugs ($n = 10$) or gelatin sponge alone in a patient with anterior spinal artery branching ($n = 1$). Eight patients died from tumor progression 10.1 ± 4.6 months later, and two patients survived 2 and 26 months, respectively. The remaining patient died of bone metastases after 32 months despite liver transplantation 10 months after chemoembolization. The right lumbar artery supplies HCC located in the bare area of the liver, especially in patients who undergo repeated chemoembolization, including chemoembolization by way of the right IPA. Chemoembolization by way of the right lumbar artery may be safe when the feeder is well selected.

Keywords Hepatocellular carcinoma · Chemoembolization · Lumbar artery supply

Introduction

Extrahepatic collateral pathways to the liver and hepatocellular carcinoma (HCC) can develop under various conditions, e.g., after interruption of the hepatic artery by surgical ligation, arterial injury induced by repeated chemoembolization procedures, or placement of a catheter [1, 2]. Adhesion between the liver and other organs exaggerates the degree of extrahepatic collaterals [3]. An extrahepatic blood supply to HCC also develops in the anatomic location of HCC, although the hepatic arterial supply remains intact [4]. Extrahepatic collateral supplies can inhibit the effectiveness of chemoembolization treatment. To ensure effective transcatheter management of HCC, these collaterals should be adequately embolized [3–12]. The right lumbar artery infrequently supplies HCC located in the bare area of the liver [5, 6]. In this report, we describe the clinical features of HCC supplied by the lumbar artery.

S. Miyayama (✉) · M. Yamashiro · M. Okuda · Y. Yoshie · N. Sugimori · S. Igarashi · Y. Nakashima
Department of Diagnostic Radiology, Fukuiken Saiseikai Hospital, Fukui 918-8503, Japan
e-mail: s-miyayama@fukui.saiseikai.or.jp

O. Matsui
Department of Radiology, Kanazawa University Graduate School of Medical Science, Kanazawa 920-8641, Japan

Published online: 30 May 2009

Materials and Methods

Patients

Between October 2002 and January 2009, 11 patients with HCC supplied by the right lumbar artery were treated with chemoembolization. During the same period, 489 patients were treated by chemoembolization; therefore, the prevalence of right lumbar artery supply to the HCC was 2.2%. There were eight men and three women, and mean patient age was 69.4 ± 8.3 years (mean ± SD) (range, 53–82). Patient characteristics are listed in Table 1. All patients had liver cirrhosis. This was related to hepatitis C in eight patients and to hepatitis B in one patient; one patient had both hepatitis B and C; HCC etiology in the remaining patient was unknown. The original tumor treated by initial chemoembolization was single nodular ($n = 5$) or multinodular ($n = 6$) and located in segment 8 ($n = 2$), segment 5 ($n = 2$), segment 7 ($n = 2$), segments 8 and 7 ($n = 2$), segments 7 and 1 ($n = 1$), segments 6 and 3 ($n = 1$), and segments 8, 7, and 6 ($n = 1$). The treatment records were retrospectively analyzed.

Classification of Hepatic Arterial Damage

Angiographic findings demonstrating the right lumbar artery supply were retrospectively analyzed. Damage to the hepatic arterial branch was divided into four grades: (1) severe, i.e., occlusion of the right or left hepatic artery; (2) moderate, i.e., occlusion of the segmental artery of the liver; (3) slight, i.e., occlusion of the subsegmental artery of the liver; and (4) none, i.e., no obvious damage to the hepatic arterial branches.

Chemoembolization Methods and Follow-Up

Written informed consent was obtained from each patient before chemoembolization was performed. Institutional Review Board approval was not required at our institution for this retrospective study. Arteriograms of the right lower intercostal arteries (T10 and T11), the subcostal artery, and the right upper lumbar arteries (L1 and L2) were routinely obtained in all patients to determine where the anterior spinal artery originated. After confirmation of the tumor-feeding branch, selective catheterization into the tumor-feeding branch using a 2F tip microcatheter (Progreat α; Terumo, Tokyo, Japan) was attempted. The embolization procedure was performed according to the following therapeutic strategies:

(1) When the tumor-feeding branch could be selected and the anterior spinal artery was not derived from the parent artery or adjacent arteries, chemoembolization was performed using gelatin sponge particles (Gelfoam; Upjohn, Kalamazoo, MI, or Gelpart; Nihon Kayaku, Tokyo, Japan) after injection of a mixture of 1 to 2 ml iodized oil (Lipiodol; Andre Guerbet, Aulnaysous-Bois, France) and anticancer drugs (10 mg epirubicin [Farmorbicin; Kyowa Hakko, Tokyo, Japan] and 2 mg mitomycin C [Mitomycin; Kyowa Hakko]).
(2) When the tumor-feeding branch could be selected and the anterior spinal artery was derived from the parent artery or adjacent arteries, the feeding branch was embolized by gelatin sponge particles alone.
(3) When the tumor-feeding branch could not be selected, the procedure was ended without embolization.

Chemoembolization was simultaneously performed not only by way of the hepatic arterial branches but also other extrahepatic collaterals if necessary.

Computed axial tomography (CAT) was performed 1 week after the procedure in all patients to determine the distribution of iodized oil. All patients but one were followed up, and tumor recurrence was judged by CAT or magnetic resonance imaging obtained every 2–3 months after chemoembolization. The remaining patient underwent follow-up CAT 1 week later only because chemoembolization had been performed 2 months previously, and further follow-up imaging was not performed.

Results

Pretreatment Findings

All patients underwent 3 to 15 chemoembolization sessions (mean 6.7 ± 3.7) before discovery of blood supply from the right lumbar artery to the HCC. The interval between initial chemoembolization and discovery of the right lumbar artery supply was 53.2 ± 26.9 months (range, 6–86). In addition, seven patients had undergone previous percutaneous local therapy (percutaneous ethanol injection [$n = 3$], microwave coagulation therapy [$n = 1$], or radiofrequency ablation [RFA] [$n = 5$]) combined with chemoembolization to the tumor fed by the right lumbar artery ($n = 2$) or other tumors ($n = 5$). One patient had undergone previous radiation therapy to the tumor fed by the right lumbar artery in addition to RFA. Another patient had a history of hepatic resection for HCC. All patients had undergone previous chemoembolization of extrahepatic collateral vessels supplying the HCC. The right inferior phrenic artery (IPA) was embolized in 10 patients. In addition, the right renal capsular artery ($n = 5$), left IPA ($n = 2$), right intercostal arteries ($n = 4$), right middle adrenal artery ($n = 2$), omental arteries ($n = 2$), cystic

Table 1 Summary of 11 patients with HCC fed by the right lumbar artery

Patient no./age/sex	No. of previous chemoembolizations	Other therapy	Tumor type/location at initial chemoembolization	Interval between initial chemoembolization and lumbar artery supply (mo)	Angiographic findings of tumor fed by lumbar artery					Outcomes
					Tumor size (cm)/location	Hepatic artery damage	Feeding artery	Feeding branches	Anterior spinal artery	
1/53/M	9	None	Multinodular/S5	82	1.5/S7	Severe	L2	Proximal[a]	–	Dead at 32 mo[b]
2/82/M	15	PEI, MCT	Multinodular/S8	86	2/S7	Severe	L1	Proximal	–	Dead at 5 mo
3/74/F	3	None	Multinodular/S7 and S1	38	1.8/S7	Moderate	L1	Proximal	–	Dead at 16 mo
4/73/M	10	PEI, RFA	Single nodular/S5	48	1.8/S7	Severe	L1	Proximal	–	Dead at 10 mo
5/79/M	6	RFA	Single nodular/S7	76	2/S7	Slight	L1	Proximal	–	Alive at 26 mo
6/68/M	6	RFA	Multinodular/S6 and S3	34	3/S6	Severe	L1	Distal[c]	–	Dead at 7 mo
7/58/M	4	None	Single nodular/S8 and S7	6	9.8/S7	Moderate	L1	Proximal	–	Dead at 13 mo
8/69/M	4	PEI	Multinodular/S8, S7, and S6	20	2.3/S7	Moderate	L1	Proximal	–	Dead at 15 mo
9/69/M	9	RFA	Single nodular/S8	78	2.8/S7	Severe	L1	Distal	–	Dead at 5 mo
10/67/F	5	RFA, RT	Single nodular/S7	49	4.3/S7	Moderate	L1	Distal	–	Dead at 7 mo
11/71/F	3	Resection	Multinodular/S8 and S7	68	3/S7	Moderate	L1	Proximal	+	Alive at 2 mo

PEI percutaneous ethanol injection, *MCT* microwave coagulation therapy, *RFA* radiofrequency ablation, *RT* radiotherapy

[a] The feeding-branch arose proximal to the bifurcation of the dorsal ramus and muscular branches

[b] This patient underwent liver transplantation 10 months after chemoembolization by way of the right lumbar artery

[c] The feeding-branch arose from the muscular branches

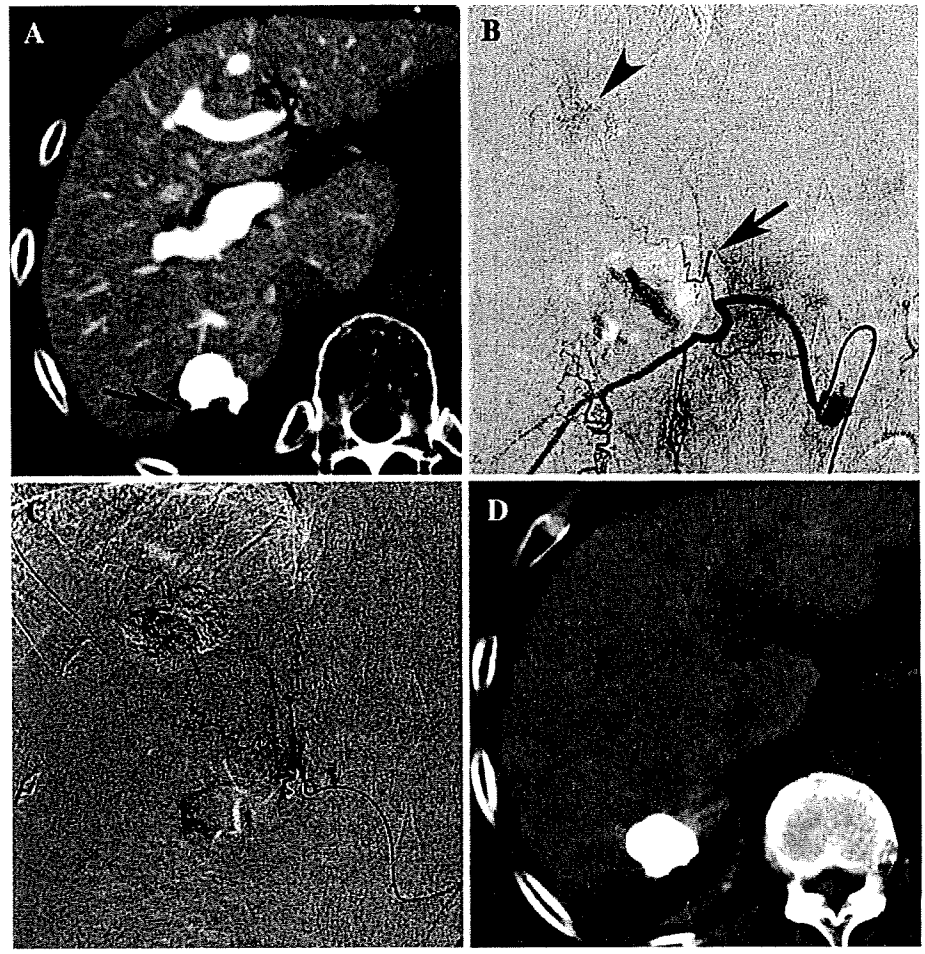

Fig. 1 A 79-year-old man with HCC supplied by the right lumbar artery (patient no. 5). (**A**) CAT during arterial portography image shows a hypoattenuating area adjacent to a defect of iodized oil accumulation at the posterior aspect of the tumor, suggesting local recurrence (*arrow*). (**B**) Arteriogram of the right first lumbar artery shows a small tumor-feeding branch arising at the proximal portion (*arrow*) and tumor stain (*arrowhead*). (**C**) The tumor-feeding branch was selected, and chemoembolization was performed. (**D**) CAT obtained 1 week after the procedure shows dense iodized oil accumulation in the recurrent tumor portion

artery ($n = 1$), middle colic artery ($n = 1$), right internal mammary artery ($n = 1$), branches of left ($n = 1$) or right gastric artery ($n = 1$), and bile duct artery ($n = 1$) were also embolized.

All patients had a single HCC that was partially ($n = 6$) or completely ($n = 5$) fed by the right lumbar artery. Ten tumors were local recurrences after chemoembolization. Six tumors were original tumors with local recurrence despite several chemoembolization procedures. Four were sequentially developed tumors at other sites with local recurrence after additional chemoembolization. The remaining tumor was a newly developed tumor at another site without any treatment. Nine patients had multiple viable tumors in addition to the tumor fed by the right lumbar artery. Two patients had a solitary tumor fed by the right lumbar artery that was the original tumor with local recurrence.

Hepatic arterial damage was found in all patients. The grades of damage were classified as severe ($n = 5$), moderate ($n = 5$), and slight ($n = 1$). None of the tumors supplied by the lumbar artery had invaded the abdominal wall, and the mean tumor diameter was 3.1 ± 2.4 cm (range 1.5 to 9.8). All except one of the tumors supplied by the right lumbar artery were located in the bare area of segment 7. The remaining tumor was located on the liver surface of segment 6 near the right renal fossa.

Chemoembolization

In 10 patients, the HCC was supplied by the right first lumbar artery (Figs. 1 through 4). In the remaining patient, the right second lumbar artery supplied the tumor because the first lumbar artery was hypoplastic. In one patient, the anterior spinal artery was derived from the tumor-feeding right first lumbar artery (Fig. 4). In the other 10 patients, the anterior spinal artery did not originate from the right lower intercostal, subcostal, or upper lumbar arteries.

A small branch arising proximal to the bifurcation of the dorsal ramus and muscular branches supplied the HCC in eight patients (Figs. 1, 3, 4). In three patients, the feeding branch was derived from the proximate portion of the muscular branches (Fig. 2). In two patients, the right IPA, which was previously embolized, was demonstrated by way of the retroperitoneal anastomosis (Fig. 3).

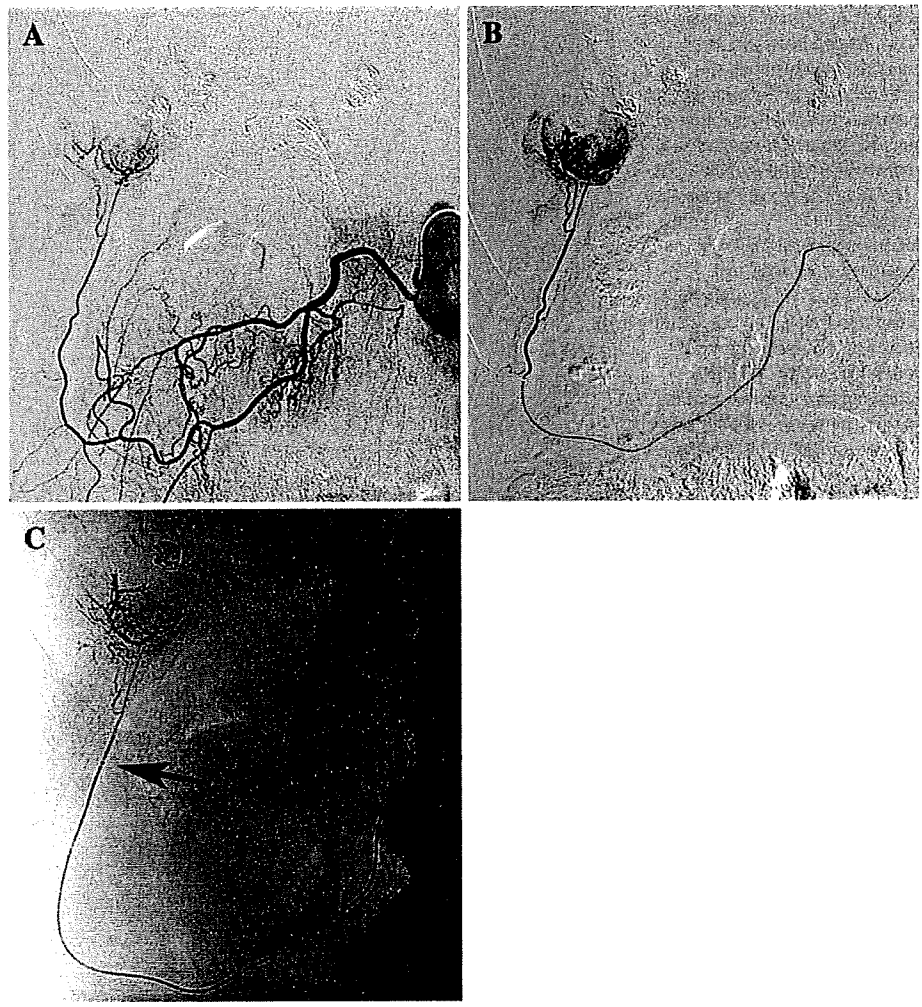

Fig. 2 A 68-year-old man with HCC supplied by the right lumbar artery (patient no. 6). (**A**) Arteriogram of the right first lumbar artery shows a tumor-feeding branch arising from the muscular branches as well as tumor stain. (**B**) The tumor-feeding branch was successfully selected. (**C**) Chemoembolization was performed at a more distal level. The catheter tip can be seen (*arrow*)

All tumor-feeding branches could be selected by the microcatheter (Figs. 1 through 4). In 10 patients, chemoembolization was performed without complications (Figs. 1 through 3). In the remaining patient whose anterior spinal artery originated from the right first lumbar artery, bland embolization was performed without complications (Fig. 4). Other extrahepatic collateral vessels were simultaneously embolized in eight patients as follows: the left gastric artery branch ($n = 1$), right intercostal arteries ($n = 3$), right IPA ($n = 1$), middle colic artery ($n = 1$), right renal capsular artery ($n = 1$), right middle adrenal artery ($n = 1$), bile duct artery ($n = 1$), and omental artery ($n = 1$). In addition, the hepatic arterial branches were embolized in 10 patients.

Outcomes

The tumor that was supplied by the right lumbar artery recurred in 9 of 10 patients at 4–9 months (4.0 ± 2.5) after chemoembolization. Four of 10 patients underwent additional chemoembolization, and the recurrent tumor was fed by the hepatic arterial branch ($n = 1$), attenuated right IPA ($n = 2$), and intercostal arteries ($n = 1$). Additional angiography was not performed in 6 patients, including one patient who underwent liver transplantation, because of diffuse tumor progression. In the remaining patient, the tumor supplied by the right lumbar artery did not recur despite progression of other tumors during the course of 4 months.

Eight patients died from tumor progression at 5–15 months (10.1 ± 4.6) after chemoembolization of the right lumbar artery. Two patients are currently alive after the procedure. One patient survived for 26 months despite two additional chemoembolization procedures for recurrent tumor. One patient survived for 2 months; however, follow-up CAT was not performed. The remaining patient, who underwent liver transplantation 10 months later, died of diffuse bone metastases 32 months after chemoembolization of the right lumbar artery.

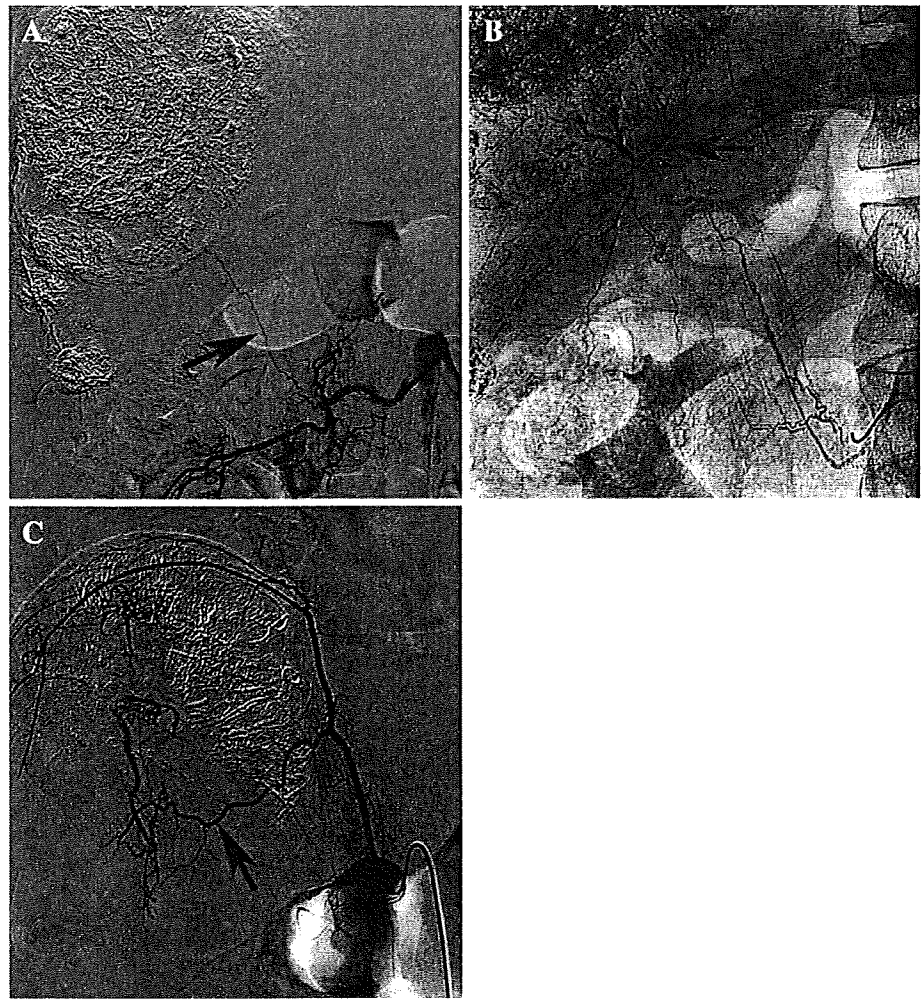

Fig. 3 A 58-year-old man with HCC supplied by the right lumbar artery (patient no. 7). (**A**) Arteriogram of the right first lumbar artery shows a tumor-feeding branch arising at the proximal portion (*arrow*). (**B**) The tumor-feeding branch was selected, and chemoembolization was performed. During the procedure, a vessel that was not seen on (**B**) was demonstrated (*arrow*). (**C**) Arteriogram obtained before right IPA chemoembolization 6 months earlier shows that the vessel is a branch of the right IPA (*arrow*)

Discussion

Various extrahepatic collaterals to HCC can develop during a subsequent course of treatment but infrequently at the initial treatment [1–12]. The right IPA is the most frequent extrahepatic collateral vessel of HCC [4–6]. The cystic artery, omental artery, internal mammary artery, intercostal artery, right renal capsular artery, left IPA, adrenal arteries, colic artery, bile duct artery, and gonadal artery are also known to develop other extrahepatic collaterals [3–12].

There are usually four lumbar arteries on each side arising from the posterior aspect of the abdominal aorta. These arteries anastomose with one another and with the lower posterior intercostal, subcostal, iliolumbar, deep circumflex iliac, and inferior epigastric arteries [13]. Three major branches derive from the lumbar artery: the dorsal ramus, spinal, and muscular branches. In the present study, a small branch arising proximal to the bifurcation of the dorsal ramus and muscular branches fed the HCC in eight patients, and small branches arising from the muscular branches fed the tumor in three patients.

In all patients, the right IPA was also embolized either previously or simultaneously. The right IPA is the major source of the diaphragmatic pathways, and the intercostal and internal mammary arteries support these pathways [9]. There are fine retroperitoneal networks between the right IPA, dorsal pancreatic artery, adrenal artery, and left gastric artery. In addition, the right lumbar artery infrequently also acts as a supportive diaphragmatic pathway [14]. Lumbar artery collateral supply occurs late, after both the hepatic and diaphragmatic circulations are severely attenuated by repeated chemoembolization. In contrast, a large tumor invading the abdominal wall may receive the blood supply from the lumbar artery without damaging the hepatic arteries and IPA [5]. Therefore, the prevalence of a lumbar artery supply may be influenced by tumor size. In our series, none of the tumors had invaded the abdominal wall, and all tumors except one were relatively small.

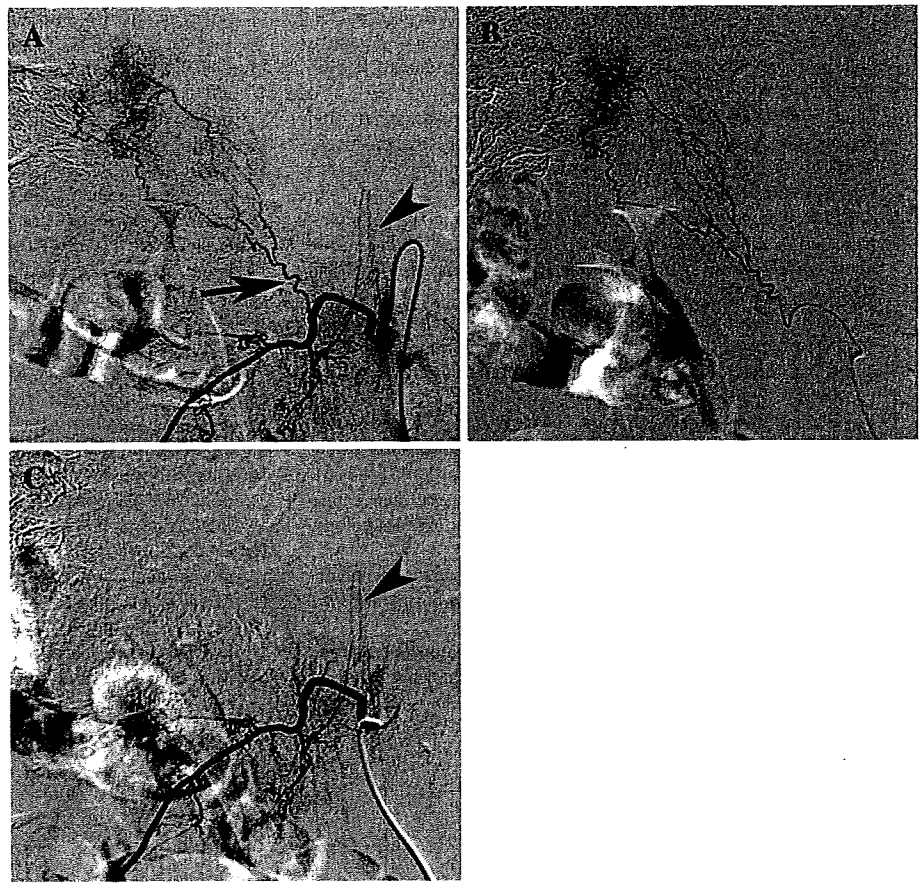

Fig. 4 A 71-year-old woman with HCC supplied by the right lumbar artery (patient no. 11). (**A**) Arteriogram of the right first lumbar artery shows a tumor-feeding branch arising from the proximal portion (*arrow*) as well as tumor stain. The anterior spinal artery is also seen (*arrowhead*). (**B**) The tumor-feeding branch was selected, and bland embolization was performed without complication. (**C**) Arteriogram obtained immediately after embolization shows that the tumor-feeding branch is embolized and the anterior spinal artery is patent (*arrowhead*)

Therefore, repeated chemoembolization procedures and tumor location at the bare area of the liver may have exaggerated the lumbar artery supply.

Inadvertent chemoembolization of the spinal or skin-feeding branches may cause spinal cord injury or skin necrosis [6, 15, 16]. Superselective catheterization into the tumor-feeding branch is necessary to safely perform chemoembolization of collateral vessels. All tumor-feeding branches were small; however, they could be selected using a 2F tip microcatheter in our series. Because the lumbar arteries anastomose with arteries from above and from below [13, 17], embolic materials may pass through these anastomoses 18]. Therefore, arteriography of the right lower intercostal, subcostal, and upper lumbar arteries should be performed before chemoembolization to confirm where the anterior spinal artery originates. Bland embolization by way of the tumor-feeding branch using gelatin sponge particles may be safe when the anterior spinal artery derives from the tumor-supplying lumbar artery or from neighboring arteries.

Efficacy of chemoembolization by way of the right lumbar artery is uncertain because the majority of our patients died within a relatively short period after chemoembolization by way of the right lumbar artery. However, one patient survived for 26 months after chemoembolization by way of the right lumbar artery despite two local recurrences. Therefore, we believe that chemoembolization by way of the right lumbar artery may prolong patient survival.

In conclusion, the right lumbar artery supplies HCC located at the bare area of the liver, especially in patients with attenuation of hepatic arterial branches by repeated chemoembolization, including by way of the right IPA. The tumor-feeding branch arises proximal to the bifurcation of the dorsal ramus and muscular branches in most cases; however, it infrequently arises from the muscular branches. Chemoembolization by way of the right lumbar artery may be safe when the tumor-feeding branch is successfully selected.

References

1. Michels NA (1953) Collateral arterial pathways to the liver after ligation of the hepatic artery and removal of the celiac axis. Cancer 6:708–724
2. Koehler RE, Korobkin M, Lewis F (1975) Arteriographic demonstration of collateral arterial supply to the liver after hepatic artery ligation. Radiology 117:49–54

3. Miyayama S, Matsui O, Akakura Y et al (2001) Hepatocellular carcinoma with blood supply from omental branches: treatment with transcatheter arterial embolization. J Vasc Interv Radiol 12:1285–1290
4. Chung JW, Park JH, Han JK et al (1998) Transcatheter oily chemoembolization of the inferior phrenic artery in hepatocellular carcinoma: the safety and potential therapeutic role. J Vasc Interv Radiol 9:495–500
5. Kim HC, Chung JW, Lee W et al (2005) Recognizing extrahepatic collateral vessels that supply hepatocellular carcinoma to avoid complications of transcatheter arterial chemoembolization. Radiographics 25(suppl):S25–S39
6. Miyayama S, Matsui O, Taki K et al (2006) Extrahepatic blood supply to hepatocellular carcinoma: angiographic demonstration and transcatheter arterial chemoembolization. Cardiovasc Intervent Radiol 29:39–48
7. Miyayama S, Matsui O, Nishida H et al (2003) Transcatheter arterial chemoembolization for unresectable hepatocellular carcinoma fed by the cystic artery. J Vasc Interv Radiol 14:1155–1161
8. Nakai M, Sato M, Kawai N et al (2001) Hepatocellular carcinoma: involvement of the internal mammary artery. Radiology 219:147–152
9. Park SI, Lee DY, Won JY et al (2003) Extrahepatic collateral supply of hepatocellular carcinoma by the intercostal arteries. J Vasc Interv Radiol 14:461–468
10. Kodama Y, Shimizu T, Endo H et al (2002) Spontaneous rupture of hepatocellular carcinoma supplied by the right renal capsular artery treated by transcatheter arterial embolization. Cardiovasc Intervent Radiol 25:137–140
11. Suh SH, Won JY, Lee DY et al (2005) Chemoembolization of the left inferior phrenic artery in patients with hepatocellular carcinoma: radiologic findings and clinical outcome. J Vasc Interv Radiol 16:1741–1745
12. Kim HC, Chung JW, Jae HJ et al (2006) Hepatocellular carcinoma: transcatheter arterial chemoembolization of the gonadal artery. J Vasc Interv Radiol 17:703–709
13. Uflacker R (1997) Atlas of vascular anatomy: angiographic approach. Williams & Wilkins, Baltimore, MD, p 418
14. Miyayama S, Matsui O, Taki K et al (2004) Transcatheter arterial chemoembolization for hepatocellular carcinoma fed by the reconstructed inferior phrenic artery: anatomical and technical analysis. J Vasc Interv Radiol 15:815–823
15. Chung JW, Park JH, Han JK et al (1996) Hepatic tumors: predisposing factors for complications of transcatheter oily chemoembolization. Radiology 198:33–40
16. Arora R, Soulen MC, Haskal ZJ (1999) Cutaneous complications of hepatic chemoembolization via extrahepatic collaterals. J Vasc Interv Radiol 10:1351–1356
17. Caglar S, Dolgun H, Ugur HC et al (2004) Extraforaminal lumbar arterial anatomoy. Surg Neurol 61:29–33
18. Miyayama S, Yamashiro M, Okuda M, et al. (2008) Anastomosis between the hepatic artery and the extrahepatic collateral or between extrahepatic collaterals: observation on angiography. J Med Imaging Radiat Oncol (in press)

Jpn J Radiol (2009) 27:53–68
DOI 10.1007/s11604-008-0299-7

REVIEW

Radiological and histopathological manifestations of hepatocellular nodular lesions concomitant with various congenital and acquired hepatic hemodynamic abnormalities

Satoshi Kobayashi · Osamu Matsui · Toshifumi Gabata
Junichiro Sanada · Wataru Koda · Tetsuya Minami
Yasuji Ryu

Received: July 19, 2008 / Accepted: October 31, 2008

Abstract Congenital and acquired hepatic hemodynamic abnormalities are classified into four categories: hepatic arterial inflow disorder, portal vein inflow disorder, hepatic vein outflow disorder, and presence of a third inflow to the liver. Although their detailed etiology is not fully understood, these hepatic hemodynamic abnormalities may cause the formation of hepatocellular nodules. Recent advances in imaging modalities now enable visualization of these hepatocellular nodules concomitantly with the identification of various congenital and acquired hemodynamic abnormalities. Most of these nodular lesions are benign hyperplastic nodules, such as focal nodular hyperplasia, nodular regenerative hyperplasia, and other types of regenerative nodules. However, neoplastic nodules such as hepatic adenoma and hepatocellular carcinoma may also occur in conjunction with hepatic hemodynamic abnormalities. Distinguishing neoplastic nodules, especially malignant liver tumors, from hyperplastic nodules is important. Detection of intranodular Kupffer cells with superparamagnetic iron oxide enhanced magnetic resonance imaging is a key indicator that a nodule is regenerative rather than neoplastic.

S. Kobayashi (✉) · O. Matsui · T. Gabata · J. Sanada · W. Koda · T. Minami · Y. Ryu
Department of Radiology, Kanazawa University School of Medicine, 13-1 Takara-Machi, Kanazawa 920-8641, Japan
Tel. +81-76-265-2323; Fax +81-76-234-4256
e-mail: satoshik@rad.m.kanazawa-u.ac.jp

Key words Portal vein · Hepatic circulation · Hepatic nodule

Introduction

Concomitant hepatocellular nodular lesions are occasionally found with various congenital and acquired hepatic vascular abnormalities including the following: congenital absence of the portal vein, idiopathic portal hypertension, and the Budd-Chiari syndrome. Although the etiology of such nodules is not fully understood, alterations in the hepatic microcirculation are thought to be closely related to nodule formation.[1,2] Histopathological studies have found that most are hyperplastic nodules, such as focal nodular hyperplasia (FNH) or nodular regenerative hyperplasia (NRH), but that rarely these nodules may be neoplastic—e.g., hepatic adenoma or hepatocellular carcinoma (HCC). Radiological studies indicate that hyperplastic nodules may have either an arterial-dominant or a portal-dominant vascular supply.

This article reviews various types of hepatic vascular and circulatory abnormalities. It then discusses the radiological and histopathological manifestations of hepatocellular nodules that occur concomitantly with these various congenital and acquired hepatic hemodynamic abnormalities.

Hepatic circulation

The liver has a dual blood supply from the portal vein and the hepatic artery. The portal vein, which supplies venous blood from the gastrointestinal organs to the

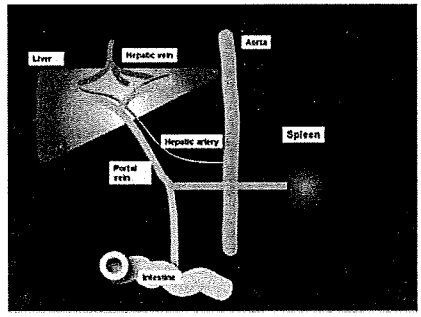

Fig. 1. Hepatic circulation. The liver has a dual blood supply, via the hepatic artery and the portal vein. Blood outflow drains into the hepatic vein. Alterations in hepatic hemodynamics occasionally cause hepatocellular nodule formation

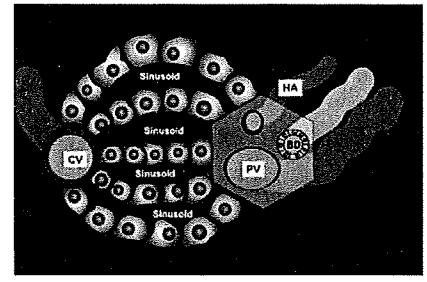

Fig. 2. Hepatic sinusoidal circulation. The terminal portal venules and hepatic arterioles run within the portal tract to create a dense network of vessels called the peribiliary plexus, from which blood flows into the sinusoid. Blood leaving the sinusoid drains into a central vein (*CV*). *HA*, terminal hepatic arteriole; *PV*, terminal portal venule; *BD*, terminal bile duct

liver, is essential to maintaining liver function (Fig. 1). Normally, the liver receives about 1500 ml of blood per minute. Based on intraoperative electromagnetic flowmetry measurements in humans and dogs, 70% of this flow derives from the portal vein and 30% from the hepatic artery.[3]

Under normal conditions, liver function thus has only limited dependence on arterial blood. However, in the event of a sudden, marked reduction in portal blood flow, arterial blood flow is able to increase acutely by an incompletely understood compensatory mechanism to prevent anoxic tissue necrosis. Conversely, portal flow is able to increase in response to a reduction in arterial flow, indicating the presence of mutually compensating mechanisms. Blood drainage from the liver occurs through the hepatic venous system, which contains four major veins: the right, left, and middle hepatic veins and the inferior right hepatic vein. The first three of these major veins enter the inferior vena cava at the level of the diaphragm. The inferior right hepatic vein, which is smaller in caliber, enters the vena cava caudally along with several other small veins.[3–5]

Microcirculation of the liver

The portal venules and hepatic arterioles flow separately into the sinusoid of the liver but also communicate with each other via a dense network of vessels around the bile duct called the peribiliary plexus, from which peribiliary efferent venules flow into the sinusoid. The plexus acts to regulate the volume of blood flow in both the portal venous system and the hepatic arterial system. While the blood supply to the liver has a dual origin, all blood leaves the liver through a single venous system: the central veins receive sinusoidal blood and then unite to form the major hepatic veins (Fig. 2).[3–5]

Table 1. Classification of hepatic vascular and circulatory abnormalities

Hepatic arterial inflow disorder
Hepatic artery stenosis/occlusion
Vasculitis/angiitis (collagen disease)
Arteriovenous shunt (Rendu-Osler-Weber disease)
Portal vein inflow disorder
Idiopathic portal hypertension
Extrahepatic portal vein occlusion/portal vein thrombosis
Congenital absence of the portal vein (complete/partial)
Intrahepatic portosystemic shunt
Hepatic vein outflow disorder
Budd-Chiari syndrome/hepatic vein thrombosis
Venoocclusive disease
Presence of the third inflow
Parabiliary venous system (aberrant right gastric vein)
Cholecystic vein
Sappey's vein

Classification of hepatic vascular and circulatory abnormalities

Depending on the affected vessel and/or site, hepatic vascular and circulatory abnormalities are classified as indicated in Table 1.

Alterations in hepatic arterial flow

Alterations in hepatic arterial blood flow generally do not cause hepatocellular nodule formation because nodule formation most often results from alterations in nutritional and humoral factors supplied to the liver by the portal system. Even hepatic artery occlusion, a potential cause of hepatic infarction, has not been reported to induce hepatocellular nodular lesions, perhaps through a compensatory increase in portal blood flow and/or the development of a collateral supply from another arterial system. However, the following

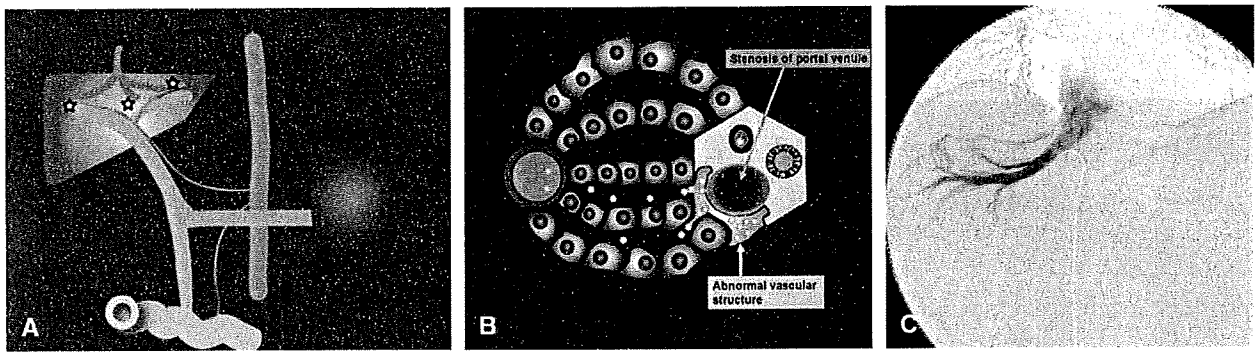

Fig. 3. Idiopathic portal hypertension (IPH). **A** Circulatory disturbance in IPH. The hepatic circulatory disturbance is observed mainly at the level of the terminal portal venules (i.e., presinusoidal level) (*star*). **B** Sinusoidal findings of IPH. The portal venule progressively shows sclerosis, stenosis, and occlusion as it finally vanishes in the portal tract. Sometimes abnormal vascular structures develop that convey collateral blood flow around the obstructed terminal portal venule. **C** Right hepatic venogram of IPH. Vein-to-vein anastomoses and the "weeping willow branches" configuration are observed

two conditions have been associated with the formation of hepatocellular nodular lesions.

Arteritis of the hepatic artery

Hepatocellular nodule formation has been observed in conjunction with several collagen diseases such as polyarteritis nodosa,[6] rheumatoid arteritis,[7–9] and systemic lupus erythematosus.[10,11] However, because the etiology of nodule formation in these diseases remains unknown, these entities are not further discussed in this article.

Hepatic arteriovenous shunt (Rendu-Osler-Weber disease)

Arteriovenous or arterioportal shunts are seen in Rendu-Osler-Weber syndrome (hereditary hemorrhagic telangiectasia).[12] Marked hepatic arterial-venous or hepatic arterial-portal shunting may cause hepatic nodule formation. Ravard et al. reported that among 24 cases of Rendu-Osler-Weber disease only one showed hepatic nodular hyperplasia on helical computed tomography (CT) examination.[13] Sinusoidal congestion and/or a disturbance in native portal venous inflow to the sinusoid due to extensive arteriovenous or arterioportal shunting may contribute to hepatocellular nodule formation.

Abnormal portal circulation

Idiopathic portal hypertension

Idiopathic portal hypertension (IPH) is defined as noncirrhotic portal hypertension in the absence of a known cause of liver disease and in conjunction with a patent extrahepatic portal vein (Fig. 3).[14–16] The etiology of IPH is still unclear. Examination of the liver reveals certain abnormalities, including areas of parenchymal atrophy due to primary portal vein sclerosis. In the atrophied areas, approximation of portal tracts and hepatic veins is apparent. Some cases show regeneration nodules, such as NRH,[17,18] perhaps in compensation for the lost parenchyma due to atrophy. Histologically, the diameter of the lumen of the portal vein is reduced. Peripheral portal tracts show fibrous enlargement and concentric periductal fibrosis. Some small portal tracts may contain no recognizable portal veins. An abnormal (aberrant) vascular structure is frequently identified around fibrosed portal tracts.

On hepatic venography, the peripheral hepatic vein branches in the right lobe are approximated and assume a configuration that resembles weeping willow branches. Vein-to-vein anastomoses develop in the periphery of the liver to produce thick anastomosing veins, perhaps as a sequela to parenchymal atrophy. Marked splenomegaly and parenchymal atrophy, especially in peripheral regions of the liver, are observed on CT and magnetic resonance imaging (MRI).

Extrahepatic portal vein obstruction/portal vein thrombosis

Extrahepatic portal vein obstruction (EHO), a frequent cause of portal hypertension in children, also occurs in adults as a result of portal thrombosis. In infants omphalitis and other forms of infection are the usual causes, whereas in adults biliary tract infection and injury to the portal vein during surgery are more commonly associated with EHO. Although the portal vein trunk is obstructed in EHO/portal vein thrombosis, portal blood

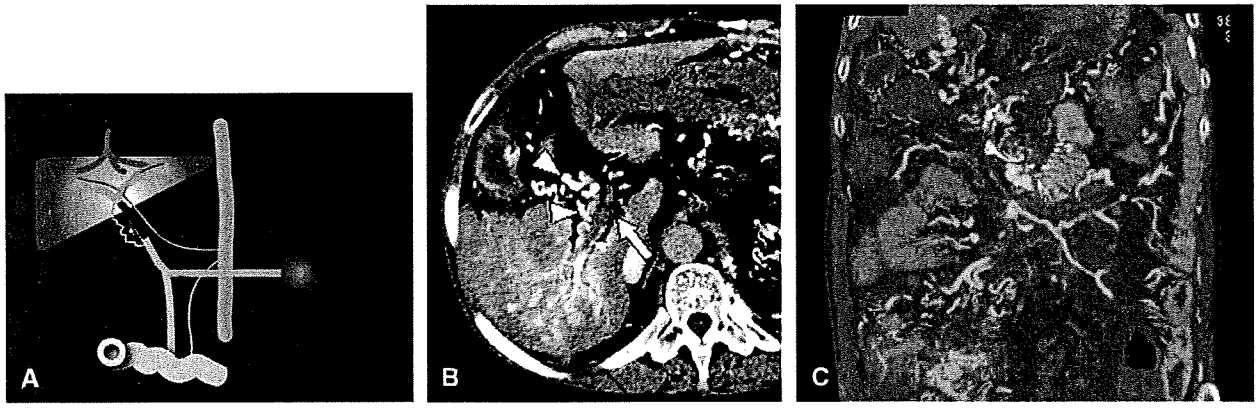

Fig. 4. Extrahepatic portal vein obstruction (EHO)/portal vein thrombosis **A** Circulatory disturbance in EHO/portal vein thrombosis. The affected site is the extrahepatic portal vein (*star*). Collateral pathways of the portal vein (cavernous transformation) develop in the hepatic hilum. **B** Computed tomography (CT) during arterial portography in a case of EHO shows right portal vein obstruction (*arrow*) and cavernous transformation of the portal vein (*arrowheads*). **C** Multiplaner reconstruction image of CT during arterial portography (CTAP) shows that the main portal vein is not opacified. Small collateral veins are observed in the hepatic hilum

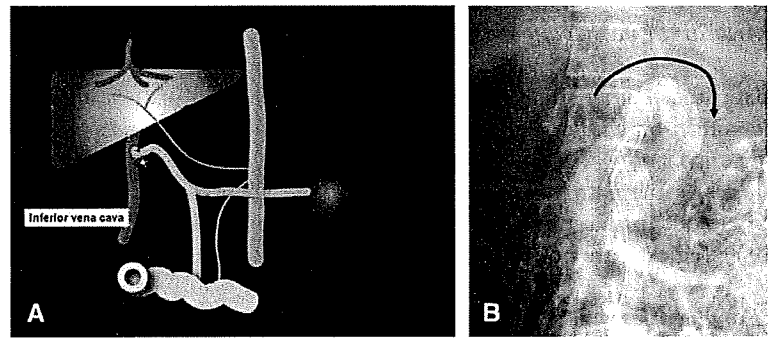

Fig. 5. Congenital absence of the portal vein. **A** Circulatory disturbances associated with congenital absence of the portal vein. The extrahepatic portal vein forms an aberrant vessel and communicates with systemic veins at various sites without drainage into the liver (indicated by *star*). **B** Portal phase image of superior mesenteric arteriography in a case of congenital absence of the portal vein. The extrahepatic portal vein forms an aberrant vessel (*curved arrow*) that communicates with the pelvic systemic vein, without drainage into the liver

flow is supplied via collateral vessels through cavernous transformation in the central part of the liver (Fig. 4). Consequently, compensatory parenchymal regeneration mainly arises in the perihilar area.[19] Scherlock et al., who first described hepatocellular nodule formation in the hepatic hilum in a case of portal vein thrombosis, named it partial nodular transformation (PNT).[20]

Congenital absence of the portal vein

Congenital absence of the portal vein is a vascular anomaly in which the portal vein is absent from the portal vein trunk to the intrahepatic branch. This leads to abnormal drainage of the mesenteric and splenic veins into the systemic circulation (Fig. 5).[21,22]

The extrahepatic and intrahepatic portal veins may not form at all, or rudimentary intrahepatic veins may be seen. Despite the lack of portal flow to the liver, patients with this anomaly usually have only mild liver dysfunction and maintain normal blood ammonia levels. Several other congenital malformations, including cardiac, visceral, and skeletal anomalies, have been associated with this condition. Congenital absence of the portal vein, with its associated reduction in portal venous blood flow, is also commonly associated with the formation of various hepatic nodules, including hyperplastic nodules,[23–26] FNH,[27–29] adenoma, HCC, and hepatoblastoma.[30]

Intrahepatic portosystemic shunt/portohepatic vein shunt

Anastomoses between the portal and hepatic veins (or inferior vena cava) have recently been demonstrated with the use of imaging modalities (Fig. 6).[31–34] Some cases show a single shunt, while others show multiple shunts. Debate continues as to whether these shunts result from an acquired change or from an embryonic anomaly. Extensive portosystemic/portohepatic shunting leads to decreased portal venous flow to peripheral liver parenchyma. Such a circulatory abnormality may

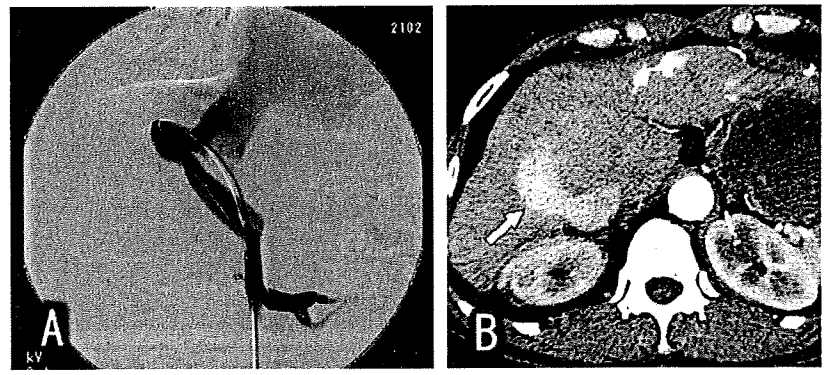

Fig. 6. Intrahepatic portosystemic shunt. **A** Portal phase image of a superior mesenteric arteriogram of an intrahepatic portosystemic shunt demonstrates no opacification of the intrahepatic peripheral portal vein branches and direct opacification of a systemic vein. **B** This early arterial phase contrast-enhanced CT scan shows a large abnormal intrahepatic vessel communicating between the main portal vein and the inferior vena cava (*arrow*)

cause compensatory regeneration of peripheral hepatic parenchyma and hepatocellular nodule formation.[35–37]

Disorders of the hepatic veins and venules (hepatic venous outflow block)

Budd-Chiari syndrome/hepatic vein thrombosis

The term Budd-Chiari syndrome (BCS) is usually applied to the clinical manifestations of hepatic venous outflow obstruction secondary to hepatic vein thrombosis. However, the term is also occasionally applied to suprahepatic obstruction of the inferior vena cava or to disease affecting small hepatic vein branches (Fig. 7).[38,39]

This syndrome may be associated with a radiological appearance suggesting membranous obstruction or stricture of the inferior vena cava. Although some early investigators believed these lesions to be developmental anomalies causing hepatic vein thromboses, recent histological and sequential radiological studies suggest that the lesions are secondary to the extension of hepatic vein thromboses.

Ultrasonography (US) studies can normally visualize the openings of the hepatic veins into the inferior vena cava. However, these openings are absent in US studies of patients with BCS, and a thrombus may manifest as intraluminal echogenicity in the hepatic vein. Other findings of BCS include an enlarged caudate lobe, splenomegaly, ascites, stenotic veins, intrahepatic collateral veins connecting with enlarged hepatic veins, vein-to-vein anastomoses, and a patent enlarged inferior right hepatic vein opening into the inferior vena cava (IVC).

Increased regenerative activity in response to continuous congestive changes in liver parenchyma causes the formation of multiple hepatocellular regenerative nodules, a histopathological appearance similar to that of FNH.[40–45] HCC may also occur in cases of BCS.[46,47]

Hepatic venoocclusive disease

Hepatic venoocclusive disease (VOD) is characterized by nonthrombotic, concentric luminal narrowing of the central or intercalated (sublobular) hepatic veins by loose connective tissue, without obstruction of large hepatic veins (Fig. 8).[48–50] These lesions are always associated with severe hemorrhagic congestion and hepatic cell necrosis affecting the central area of the lobules. The disease can progress to extensive central fibrosis with central-to-central or central-to-portal bridging, nodular regeneration, and ultimately cirrhosis. Pyrrolizidine alkaloids, irradiation, antineoplastic drugs, and immunosuppression prior to bone marrow transplantation are the main causes of VOD. VOD sometimes coexists with NRH.[51,52]

Third inflow to the liver

The presence of aberrant veins supplying small areas of liver tissue and communicating with intrahepatic portal vein branches can cause focal decreases in portal vein perfusion resulting in areas of fat sparing or fat accumulation (Fig. 9).[53]

Classification of the third inflow to liver

The third inflow to the liver was described by Matsui et al. in 1994.[54]

- *Aberrant right gastric vein (parabiliary venous system)*: The parabiliary venous system arises from the head of the pancreas, the duodenum, and the pylorus to form a network of veins within the hepatoduodenal ligament. Some of these veins flow directly into the liver (mainly the posterior part of segment IV, occasionally segment I, and less frequently segments II and III).[55]

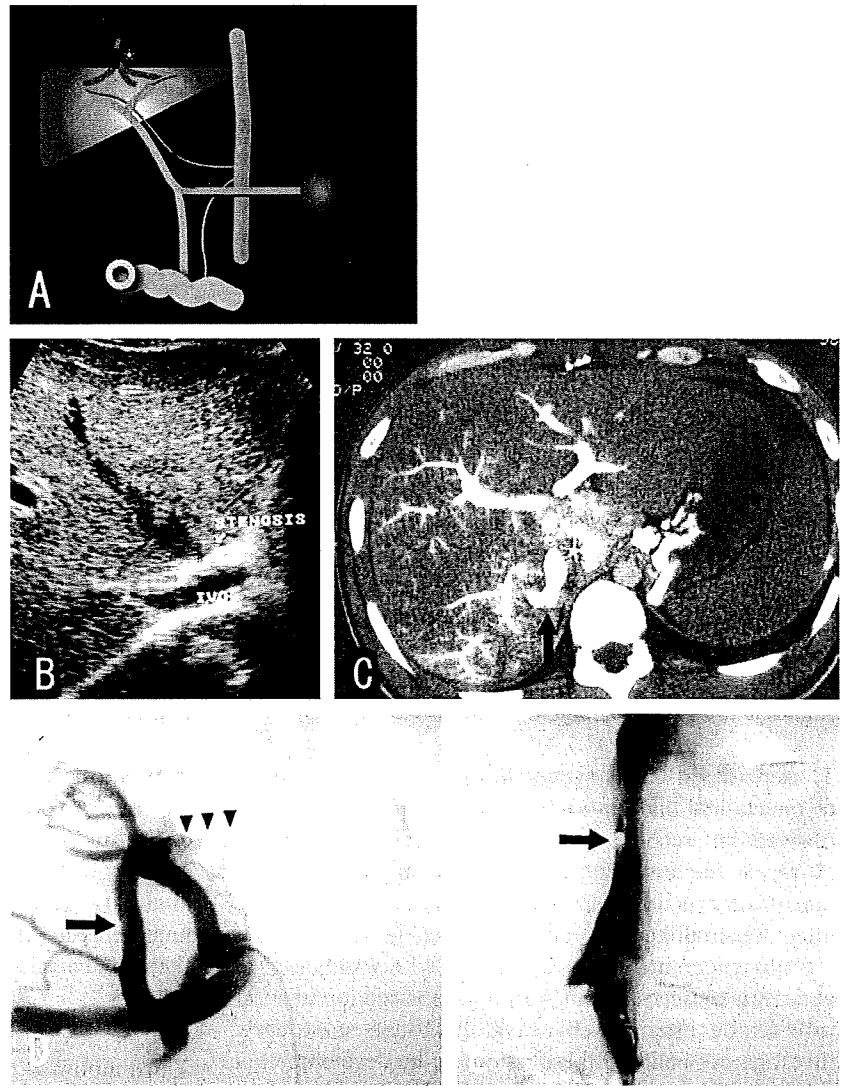

Fig. 7. Budd-Chiari syndrome. **A** Circulatory disturbance in Budd-Chiari syndrome. Obstruction of the hepatic vein and/or inferior vena cava causes hepatic congestion (*star*). **B** Axial ultrasonography image shows stenosis of the hepatic vein. **C** CTAP shows opacification of the small intrahepatic portal vein branch and irregular hepatic parenchymal staining, findings that indicate congestion of the portal vein. Communication between the inferior right hepatic vein and the inferior vena cava (IVC) is observed *(arrow)*. **D** Inferior right hepatic venogram demonstrates intrahepatic vein-to-vein anastomosis (*arrow*) and no opacification of right hepatic vein (*arrowheads*). **E** Inferior vena cavogram demonstrates stenosis of the IVC (*arrow*)

- *Cholecystic veins*: The cholecystic veins drain the cystic arteries and flow directly into the liver (mainly to segments IV and V around the gallbladder and less frequently to other segments) or communicate with the parabiliary venous system and the extrahepatic portal venous system.[56]
- *Epigastric-paraumbilical venous system*: Small veins around the falciform ligament drain the anterior part of the abdominal wall directly into the liver.
- *Superior vein of Sappey*: This vein drains the upper portion of the falciform ligament and the medial part of the diaphragm; it subsequently enters branches of the peripheral left portal vein. It communicates with the superior epigastric and internal thoracic veins.
- *Inferior vein of Sappey*: This vein drains the lower portion of the falciform ligament and enters peripheral left portal vein branches. It communicates with branches of the inferior epigastric vein around the umbilicus.
- *Vein of Burow*: This vein terminates in the middle portion of the collapsed umbilical vein and communicates with branches of the inferior epigastric vein around the umbilicus.
- *Intercalary veins*: These veins interconnect the vein of Burow and the inferior vein of Sappey.

Among these various third inflow patterns, the drainage areas of the parabiliary venous system, the veins of Sappey, and the cholecystic vein may show focal fat deposits or focal sparing of a fatty liver. Additionally, the parabiliary venous system and cholecystic venous drainage areas may show focal hyperplastic changes in cirrhotic livers.[57]

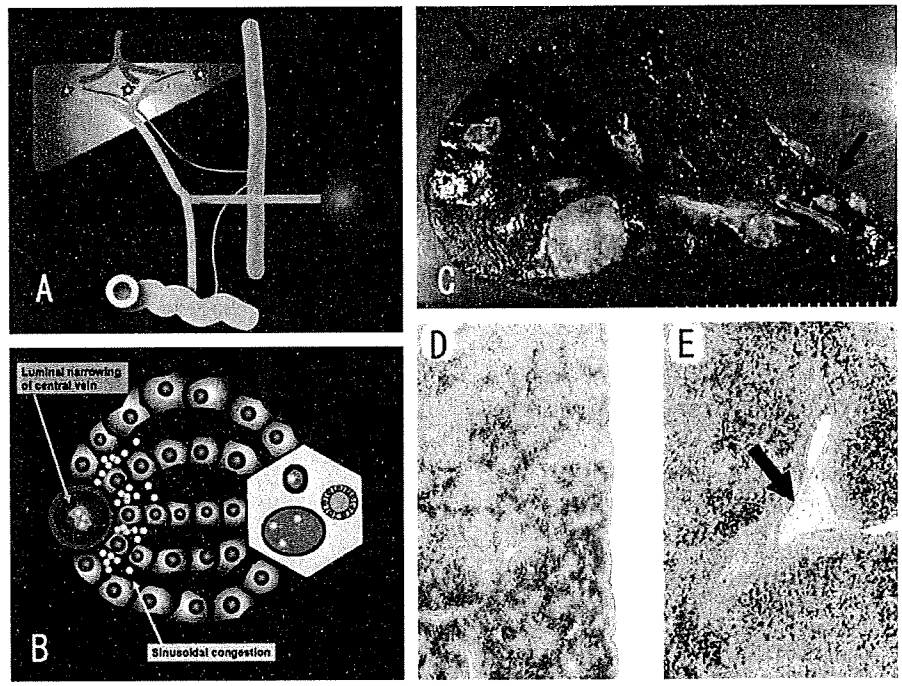

Fig. 8. Hepatic venoocclusive disease (VOD). **A** Circulatory disturbance in VOD. In VOD, the hepatic circulatory disturbance occurs primarily at the central vein level (*stars*). **B** Sinusoidal findings of VOD. The central vein of the hepatic lobule shows concentric luminal narrowing leading to sinusoidal congestion. **C** Macroscopic findings of VOD after irradiation. The right lobe and the lateral lobe of the liver are dark red (*arrows*), findings indicative of focal congestion of the liver. **D** Microscopic findings of VOD after irradiation (low magnification). The irradiated area shows marked centrilobular congestion and hemorrhage. **E** Microscopic findings of VOD after irradiation (higher magnification). The central vein shows nonthrombotic concentric luminal narrowing (*arrow*). (**D**, **E** Azan stain)

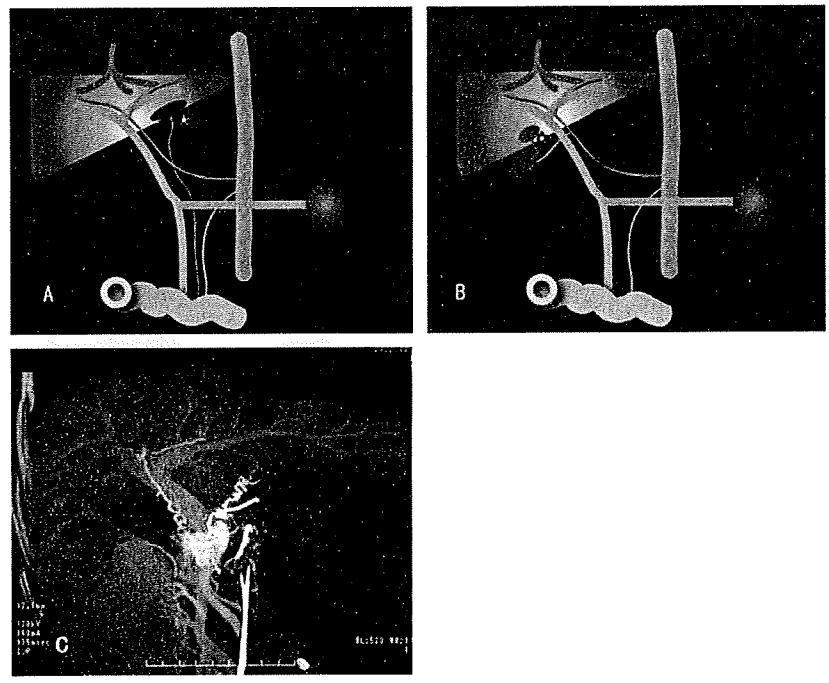

Fig. 9. Third inflow to the liver. **A** Circulatory disturbance in the aberrant right gastric vein (parabiliary venous system) drainage area. Venous flow draining directly into the hepatic parenchyma of the posterior aspect of segment IV causes a focal decrease in portal vein perfusion in the area (*star*). **B** Circulatory disturbances in the cholecystic vein drainage area. Cholecystic veins may drain directly into liver segments IV and V, which may cause focal decreases in portal vein perfusion in these areas. **C** Maximum intensity projection (MIP) image of CTAP shows parabiliary venous flow entering directly into the liver without connecting to the main portal vein

Classification of hepatocellular nodules

Table 2 describes hepatocellular nodules in accordance with the current classification system developed by the International Working Party.[58] Hepatocellular nodules occurring concomitantly with hepatic hemodynamic abnormalities are discussed in the following sections.

Monoacinar regenerative nodule (including nodular regenerative hyperplasia)

A regenerative nodule is a well-defined region of liver parenchyma that has enlarged in response to necrosis, altered circulation, or other stimuli. A monoacinar regenerative nodule involves no more than one portal

tract. Monoacinar nodules usually occur at multiple sites and can involve most of the liver as diffuse nodular hyperplasia (DNH). When DNH occurs in the absence of fibrous septa, it is also known as nodular regenerative hyperplasia (NRH) (Fig. 10).[7–9]

Diffuse nodular hyperplasia most commonly develops as a response to portal vein obstruction and may occur in noncirrhotic as well as cirrhotic livers. Monoacinar regenerative nodules also occur in other conditions with disturbed circulation, such as primary lesions of the hepatic veins or sinusoids, but the nodules associated with these conditions are less uniformly distributed or are accompanied by more congestion and more fibrous septation compared with the classic appearance of NRH.

Nodular regenerative hyperplasia is characterized by the presence of small regenerative nodules throughout the liver. The tissue between nodules is atrophic, without formation of fibrous septa. NRH is associated with a wide spectrum of systemic diseases. It has been theorized that nodule formation in NRH is a response to reduced portal blood flow as a result of peripheral portal vein thromboses. The nodules are composed of benign-appearing hepatocytes arranged in plates one to two cells thick. Many small portal veins are obliterated as a result of inflammation. The size and distribution of the nodules are variable owing to the irregular distribution of portal vein thromboses.

Typical imaging findings of NRH are as follows: hyperintensity on T1-weighted MRI, hyperdensity on CT during arterial portography (CTAP), and iso- to hypointensity on superparamagnetic iron oxide (SPIO)-enhanced T2-weighted MRI.[59–61]

Table 2. Classification of hepatocellular nodules

Regenerative lesions
Monoacinar regenerative nodule
Multiacinar regenerative nodule
Lobar or segmental hyperplasia
Cirrhotic nodule
Focal nodular hyperplasia
Dysplastic or neoplastic lesions
Hepatocellular adenoma
Dysplastic focus
Dysplastic nodule
Hepatocellular carcinoma

Fig. 10. Nodular regenerative hyperplasia (NRH) in a patient with idiopathic portal hypertension. **A** T1-weighted magnetic resonance imaging (MRI) of the liver shows a slightly hyperintense nodule in the lateral segment of the liver (*arrow*). **B** On CTAP, this nodule appears hyperdense relative to the surrounding liver (*arrow*). **C** On an early arterial phase contrast-enhanced CT scan, the nodule appears hypodense relative to the surrounding liver (*arrow*)

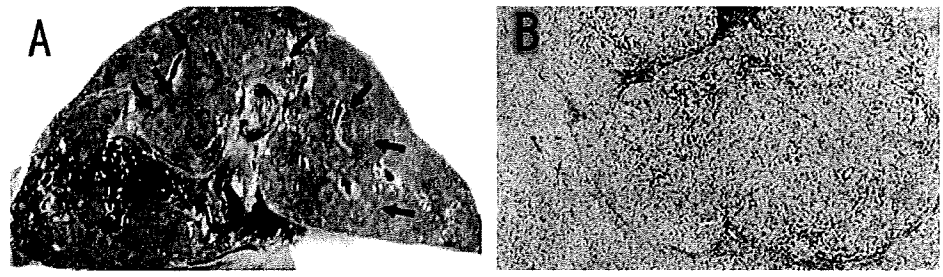

Fig. 11. Partial nodular transformation (PNT) of the liver with portal vein thrombosis. A Macroscopic findings of an autopsy specimen with PNT. Many yellow-white nodules are present around the portal tract in the hilar area (*arrows*). B Microscopic findings of the nodule. The nodule is composed of hyperplastic hepatocytes without fibrous septation involving a portal tract. The tissue between nodules shows atrophy. Histopathologically, this lesion was diagnosed as PNT. (Silver stain of reticulin fibers)

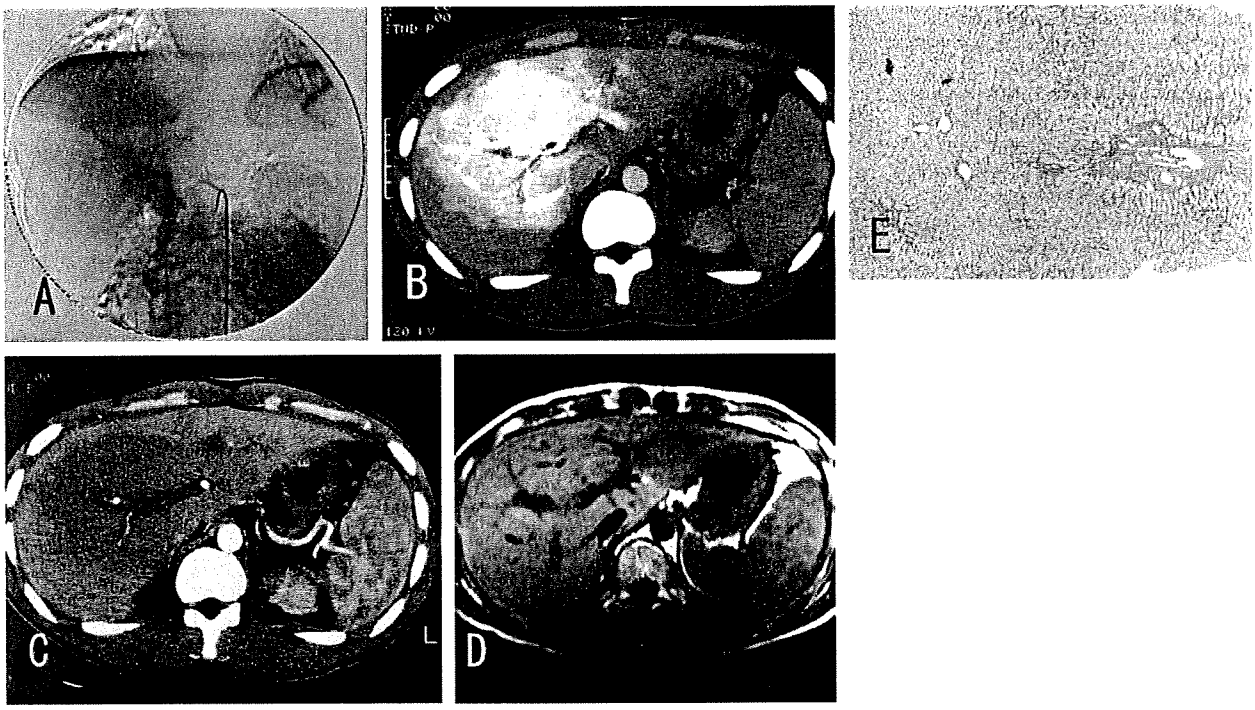

Fig. 12. Central hypertrophy of the liver in a patient with portal vein thrombosis. A Portal phase image from superior mesenteric arteriography in a patient with portal vein thrombosis. The extrahepatic portal vein is not opacified clearly, and collateral veins (i.e., cavernous transformation) are observed. B On CTAP, portal flow is shown to be preserved around the larger portal vein in the hilar area, and the peripheral liver shows portal flow defects. C Early arterial phase contrast-enhanced CT scan shows peripheral enhancement, and the perihilar area appears hypodense. D On T1-weighted MRI, the perihilar area appears slightly hyperintense relative to the peripheral area, E Needle biopsy specimen of the perihilar area revealed hyperplastic hepatocytes around the portal tract and atrophic tissue around the centrilobular area. These pathological findings resemble those of NRH and PNT. This pattern of central hypertrophy with parenchymal changes after portal vein thrombosis falls within the spectrum of PNT. (Silver stain of reticulin fibers)

Multiacinar regenerative nodules (including partial nodular transformation)

A multiacinar regenerative nodule involves more than one portal tract. These nodules usually occur at multiple sites in patients with cirrhosis or other severe diseases of the portal veins, hepatic veins, or sinusoids. When surrounded by fibrous septa, the nodules are synonymous with cirrhotic nodules. When multiacinar regenerative nodules are distinctly larger than most cirrhotic nodules within the same liver (i.e., generally at least 5 mm in diameter), they are alternatively called large regenerative nodules or macroregenerative nodules.

Partial nodular transformation (PNT) of the liver is a rare nodular lesion consisting of hyperplastic hepatocytes without significant fibrosis. Most cases of PNT have occurred at the hepatic hilum or around the large portal tract (Figs. 11, 12).[20,62,63] PNT is usually associated with portal hypertension and portal vein thrombosis. Intrahepatic portal flow disturbance and compensatory hypertrophy of the relatively less damaged parts of the liver have been postulated as possible causes of PNT.

Typical imaging findings of PNT are as follows: hyperintensity on T1-weighted MR image, hyperdensity on CTAP, and iso- to hypointensity on SPIO-enhanced T2-weighted MRI.

Hyperplastic changes

Hyperplastic changes in cirrhotic patients are sometimes seen in areas supplied by drainage from aberrant gastric veins rather than from the portal vein. In some cases of alcoholic cirrhosis, hyperplastic changes protruding into the gallbladder bed have been observed in areas directly supplied by the cystic vein (Fig. 13). These areas of hyperplastic change are hypoechoic on US, hypoattenuated on enhanced CT, hyperintense on T1-weighted MRI or hypointense on T2-weighted MRI, hypodense on CTAP, and iso- to hypointense on SPIO-enhanced T2-weighted MRI.[53,58,64] Histopathologically, the hyperplastic areas appear relatively normal compared with the remainder of the cirrhotic parenchyma. Differences in

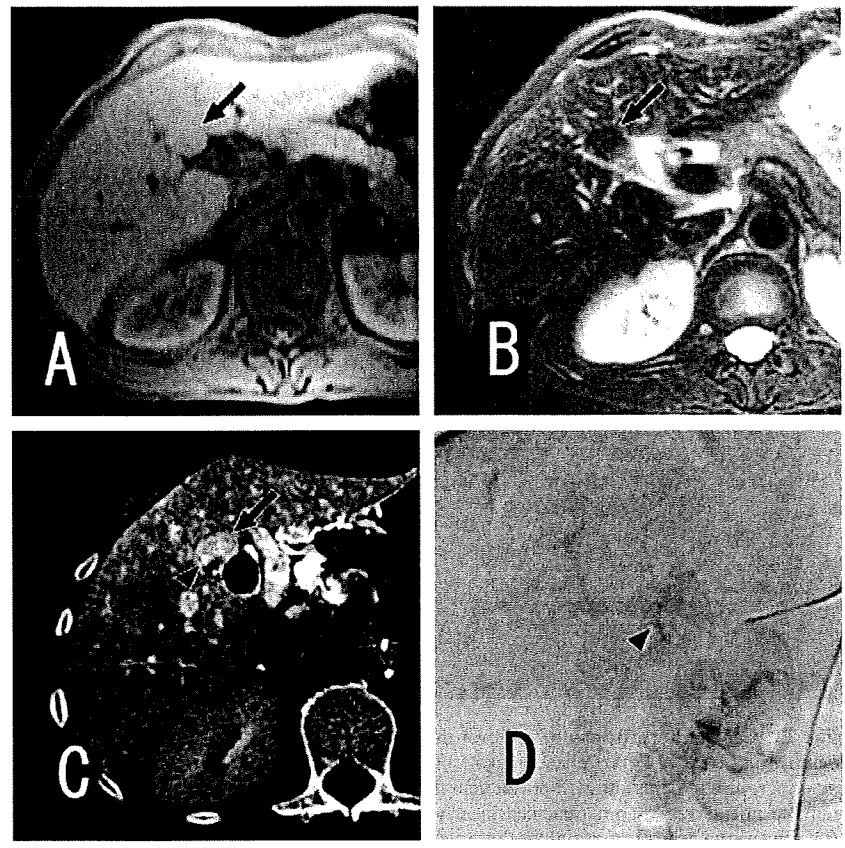

Fig. 13. Hyperplastic change in the cystic venous drainage area in a patient with alcoholic cirrhosis. **A** Fat suppressed T1-weighted MRI shows a hyperintense mass in the gallbladder fossa. **B** On superparamagnetic iron oxide (SPIO)-enhanced T2-weighted MRI, the mass lesion appears hypointense relative to the surrounding liver. **C** On CT during hepatic arteriography, the mass lesion shows enhancement, and cystic venous opacification is observed. **D** On the venous phase image of common hepatic arteriography, drainage from the cystic vein to the liver is observed (*arrowhead*)

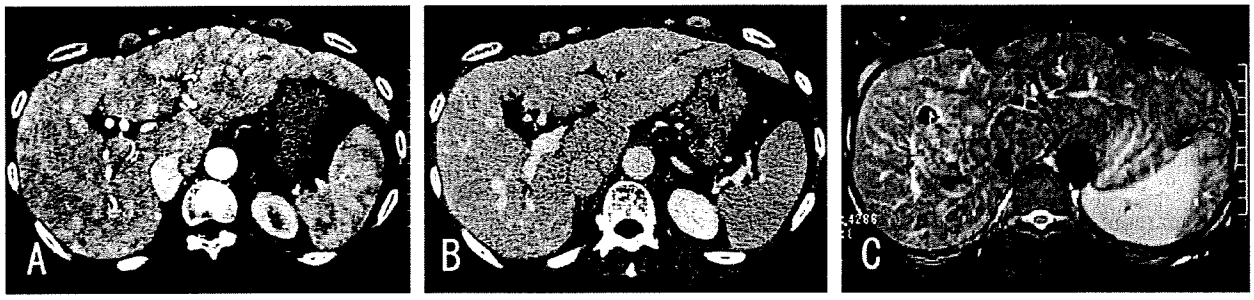

Fig. 14. Multiple focal nodular hyperplasia (FNH) in a patient with partial absence of the portal vein. **A** Early arterial phase contrast-enhanced CT scan shows multiple enhanced mass lesions, most of which contain a central hypervascular area with a peripheral hypovascular rim. **B** Portal phase contrast-enhanced CT scan shows absence of the left portal vein. Multiple mass lesions observed on early arterial phase contrast-enhanced CT appear isodense relative to the liver. **C** T2-weighted MRI shows multiple hyperintense masses with hypointense rims. On needle biopsy specimen, some of the nodules were histopathologically proven to be FNH

the concentration of some nutritional and/or hormonal factors in the blood flow may be responsible for these focal hyperplastic changes.

Focal nodular hyperplasia

Focal nodular hyperplasia is an unencapsulated, well-circumscribed, benign liver mass characterized by a central scar and surrounding nodules of hyperplastic hepatocytes. The cut surface typically reveals a central stellate fibrous scar containing one or more large arteries, often with abundant intimal or medial fibromuscular proliferation.[65–67] FNH can be diagnosed from imaging studies on the basis of its distinctive vascular anatomy and hemodynamic characteristics (i.e., a central radiating scar and increased arterial blood flow that radiates

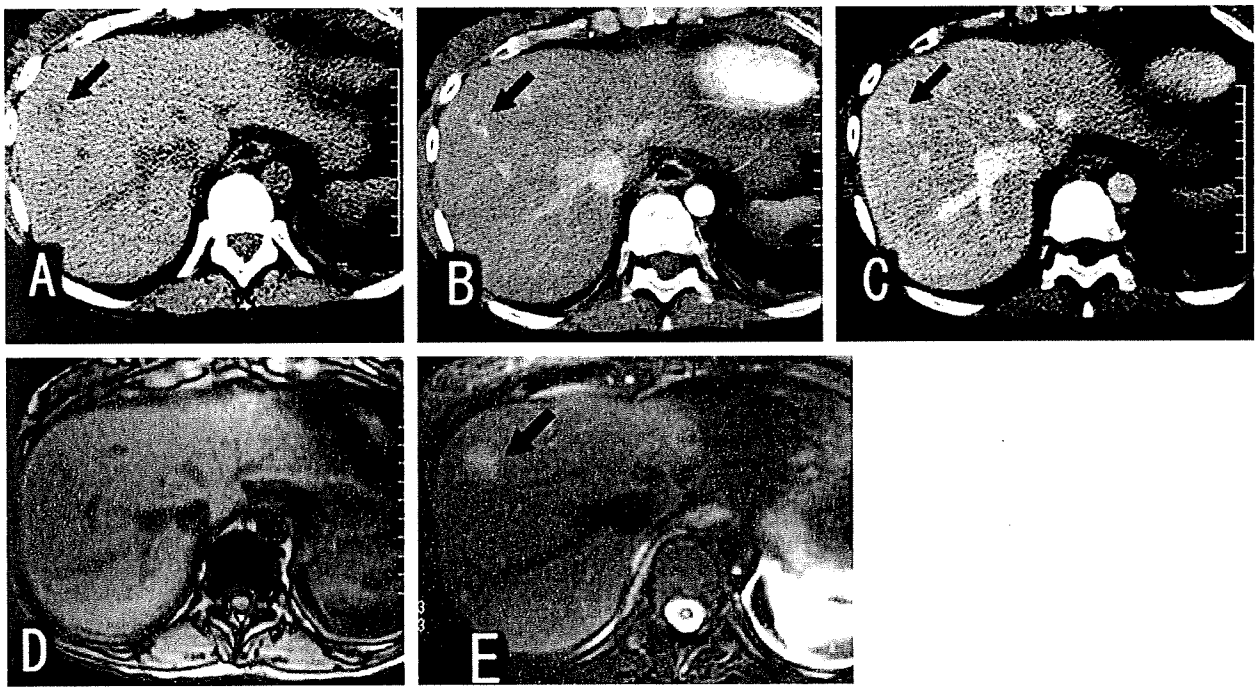

Fig. 15. Regenerative nodules in a patient with collagen disease (arteritis). A Precontrast CT shows a hypodense nodule in the right lobe of the liver (*arrow*). B On an early arterial phase contrast-enhanced CT scan, the nodule shows enhancement compared to the surrounding liver (*arrow*). C On a portal phase contrast-enhanced CT scan, the nodule appears slightly hypodense relative to the surrounding liver (*arrow*). D On T1-weighted MRI, the nodule is isointense. E On T2-weighted MRI, the nodule appears hyperintense relative to the surrounding liver (*arrow*). This nodule was diagnosed by needle biopsy as a regenerative nodule, consistent with focal nodular hyperplasia or nodular regenerative hyperplasia

Fig. 16. Regenerative nodule in Budd-Chiari syndrome. A Precontrast CT shows multiple mass lesions in the liver. B On an early arterial phase contrast-enhanced CT scan, these masses show marked enhancement. C On a portal phase contrast-enhanced CT scan, these masses show mild enhancement relative to the surrounding liver

from the center).[68,69] Radiologically, FNH shows iso- to hypointensity on T1-weighted MRI and hypodensity on CTAP. The parenchymal portion of FNH contains Kupffer cells, which take up Kupffer cell-specific MRI agents such as SPIO (Figs. 14–16). On single-level dynamic CT during hepatic arteriography (SLD-CTHA), the blood flow of small FNH drains to dilated veins in or near the nodule and surrounding hepatic sinusoid.[70] Hypervascular regenerative nodules in BCS are histopathologically similar to FNH and are thought to be a variant of FNH.

Hepatocellular adenoma

Hepatocellular adenoma is a rare benign tumor that occurs almost exclusively in women of reproductive age.[71–74] It is extremely rare in children and in men unless they are taking anabolic steroids. Kupffer cell-specific

MRI agents such as SPIO generally show no uptake in hepatocellular adenoma (Fig. 17).[75–77]

Typical imaging findings of hepatic adenoma are as follows: hyperintensity on T1-weighted MRI, hypodensity on CTAP, and hyperintensity on SPIO-enhanced T2-weighted MRI. Occasionally, FNH and adenoma coexist within the same liver. In such cases, SPIO-enhanced MRI findings are helpful for distinguishing between these two lesions.

Hepatocellular carcinoma

Hepatocellular carcinoma is a malignant neoplasm composed of tumor cells of hepatocellular origin. A small

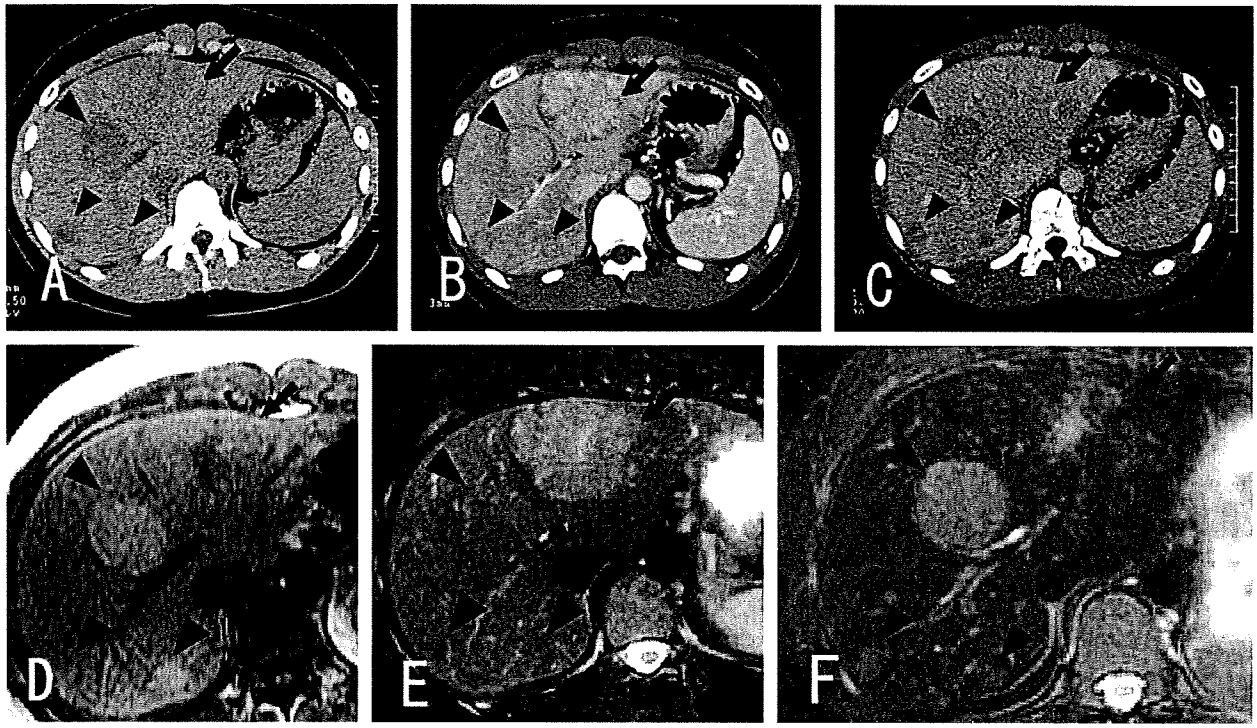

Fig. 17. Multiple focal nodular hyperplasia (FNH) and hepatic adenoma in a patient with congenital absence of the portal vein. **A** Precontrast CT shows multiple mass lesions in the liver (*arrow* and *arrowheads*). **B** Early arterial phase contrast-enhanced CT scan shows an irregular (spoke-like) enhancing mass with a peripheral hypodense rim (*arrow*) in the lateral segment of the liver and mildly enhancing masses (*arrowheads*) in the right and medial segments of the liver. **C** On a portal phase contrast-enhanced CT scan, the mass in the lateral segment revealed slight enhancement (*arrow*), whereas other masses (*arrowheads*) appeared hypodense relative to the liver. The intrahepatic portal vein is not recognized. **D** On T1-weighted MRI, the mass in the lateral segment of the liver appeared isointense (*arrow*), and the others (*arrowheads*) appeared slightly hyperintense. **E** On T2-weighted MRI, the mass in the lateral segment of the liver appeared slightly hyperintense (*arrow*), and the others (*arrowheads*) appeared isointense. **F** On SPIO-enhanced T2-weighted MRI, the mass in the lateral segment of the liver was isointense (*arrow*), and the others (*arrowheads*) were hyperintense relative to the liver. The mass with SPIO uptake (*arrow*) was diagnosed as FNH, and the masses without SPIO uptake were diagnosed as hepatic adenomas. These findings were histopathologically confirmed in needle biopsy specimens

Fig. 18. Multiple focal nodular hyperplasia (FNH) and hepatocellular carcinoma (HCC) in a patient with congenital absence of the portal vein. **A** On T1-weighted MRI, a large hypointense mass with a hyperintense rim is observed in the lateral segment of the liver (*arrow*). A small mass with a similar signal intensity pattern is seen in the medial segment of the liver (*arrowhead*). **B** On T2-weighted MRI, these masses appear hyperintense with peripheral hypointense rims (*arrow* and *arrowhead*). Radiologically, these masses were diagnosed as regenerative nodules, as in FNH. **C** Macroscopic findings of the mass resected from the lateral segment. To prevent rupture of the mass, the large mass in the lateral segment was resected. Fibrous scar is observed in the central part of the mass (*). **D** Microscopic findings of the mass resected from the lateral segment. On microscopy, a fibrous scar (*arrow*) containing a large artery was surrounded by hyperplastic hepatocytes; this mass was diagnosed as FNH. (H&E) **E** T1-weighted MRI of the liver 5 years after liver resection showed a large hypointense mass with a hyperintense rim in the medial segment of the liver (*arrowhead*). **F** On T2-weighted MRI, the mass appeared hyperintense with a peripheral hypointense rim (*arrowhead*). Comparing this image with the studies performed 5 years earlier, this mass was considered to be the same mass as the smaller mass in the medial segment of the liver that was radiologically diagnosed as FNH at that time. **G** Autopsy findings of the liver. Multiple masses were observed on the cut surface of the liver. **H** Histopathologically, the mass was diagnosed as moderately to poorly differentiated HCC. (H&E)